



UNIVERSITAT POLITÈCNICA
DE CATALUNYA
BARCELONATECH



High accuracy Synthetic Aperture Radar (SAR) Processor for UAV platforms

A Degree Thesis

Submitted to the Faculty of the

**Escola Tècnica d'Enginyeria de Telecomunicació de
Barcelona**

Universitat Politècnica de Catalunya

by

Ricard Rodríguez Torrecillas

In partial fulfilment

**of the requirements for the degree in
Telecommunication Systems Engineering**

Advisor: Antoni Broquetas Ibars

Barcelona, October 2018

Abstract

The combination of frequency-modulated continuous-wave (FMCW) technology and synthetic aperture radar (SAR) techniques leads to lightweight cost-effective imaging sensor of high resolution. One limiting factor to use of FMCW sensors is the well-known presence of nonlinearities in the transmitted signal. This results in contrast when the system is intended for high-resolution long-range applications, as it is the case for SAR.

There are many algorithms to implement SAR formation but in this case the system it is placed in a UAV (UPC ARBRES system). The large dynamics and instability characteristics of drone UAV produce large defocusing and loss of detail in the SAR images.

In this project is presented an algorithm to form synthetic apertures and compensate the defocusing and other aspects that are produced by the motion of the system. Firstly, the system it is assuming the *Stop and Go* assumption. Finally, the algorithm generates the raw data and the SAR image without assuming *Stop and Go*.

Resum

La combinació de la tecnologia d'ona continua modulada en freqüència (FMCW, per les seves sigles en anglès) i la tecnologia de radar d'obertura sintètica (SAR, per les seves sigles en anglès) condueix a un sensor d'alta resolució, lleuger i econòmic. Una limitació per a l'ús de sensors FMCW és la presència coneguda de no-linialitats en el senyal transmès. D'altra banda, contrasta quan el sistema està dissenyat per a aplicacions de llarg abast d'alta resolució, com és el cas de SAR.

Hi ha molts algorismes per implementar la formació d'imatges SAR, però en aquest cas el sistema es col·loca en un UAV (sistema UPC *ARBRES). La gran dinàmica i les característiques d'instabilitat dels avions no tripulats UAV produeixen gran desenfoqui i pèrdua de detall en les imatges SAR.

En aquest projecte es presenta un algorisme per formar obertures sintètiques i compensar el desenfoqui i altres aspectes que són produïts pel moviment del sistema. En primer lloc, el sistema està assumint el supòsit de *Stop and Go*. Finalment, l'algorisme genera les dades i la imatge *SAR sense assumir *Stop and Go*.

Resumen

La combinación de la tecnología de onda continua modulada en frecuencia (FMCW, por sus siglas en inglés) y la tecnología de radar de apertura sintética (SAR, por sus siglas en inglés) conduce a un sensor de alta resolución, liviano y económico. Una limitación para el uso de sensores FMCW es la presencia conocida de no linealidades en la señal transmitida. Por otro lado, contrasta cuando el sistema está diseñado para aplicaciones de largo alcance de alta resolución, como es el caso de SAR.

Hay muchos algoritmos para implementar la formación de imágenes SAR, pero en este caso el sistema se coloca en un UAV (sistema UPC ARBRES). La gran dinámica y las características de inestabilidad de los aviones no tripulados UAV producen gran desenfoque y pérdida de detalle en las imágenes de SAR.

En este proyecto se presenta un algoritmo para formar aberturas sintéticas y compensar el desenfoque y otros aspectos que son producidos por el movimiento del sistema. En primer lugar, el sistema está asumiendo el supuesto de *Stop and Go*. Finalmente, el algoritmo genera los datos y la imagen SAR sin asumir *Stop and Go*.

Acknowledgements

I would like to thank to professor Antoni Broquetas for his help and support. Also, for all the references that he has gave me provided and finally for his empathy to accept this project request.

Last, I would like to thank my family and my partner, for their encouragement all through this project.

Revision history and approval record

Revision	Date	Purpose
0	23/07/2018	Document creation
1	01/10/2018	Document revision

DOCUMENT DISTRIBUTION LIST

Name	e-mail
Ricard Rodríguez Torrecillas	ricard.rodriguez.torrecillas@alu-etsetb.upc.edu
Antoni Broquetas Ibars	broquetas@tsc.upc.edu

Written by:		Reviewed and approved by:	
Date	01/10/18	Date	05/10/18
Name	Ricard Rodríguez Torrecillas	Name	Anotni Broquetas Ibars
Position	Project Author	Position	Project Supervisor

Contents

1. Chapter 1 Introduction	8
1.1. General Overview.....	8
1.2. Project Goals.....	9
2. Chapter 2 Frequency Modulated Continuous Wave Radar	10
2.1. Basic operating principles and theory	10
2.2. Linear FM Signal	11
2.3. Theoretical performance.....	13
2.4. Principles using phase measurement, time discrete version.....	14
2.5. Pulse Compression FMCW	17
3. Chapter 3 Synthetic Aperture Radar Concepts.....	18
3.1. SAR Geometry	18
3.2. SAR Range equation.....	19
4. Chapter 4 Development: SAR Backprojection Algorithm.....	20
4.1. Case 1: Stop-and-Go	22
4.2. Case 2: Non-Stop-and-Go	28
4.3. Case 3: Backprojection correction for non stop-and-go	31
5. Conclusions and future development:.....	32
Bibliography:.....	33
Glossary	34

List of Figures

1. Schematic presentation RF signal	12
2. Bloc Diagram of quadrature demodulator	15
3. Frequency ramp	16
4. SAR Geometric model	18
5. SAR processing	19
6. SAR Geometric model development	20
7. Time domain raw data	24
8. Time domain phase , raw data	24
9. Compressed data	25
10. Matrix compressed data	25
11. Phase compressed data	26
12. Matrix phase compressed data	26
13. SAR image case 1	27
14. Range and Azimuth case 1.....	28
15. Radial velocity	29
16. Compressed data Stop and Go vs Non Stop and Go	30
17. SAR image case 2	30
18. SAR image case 3	31
19. Range and Azimuth case 3	31

Chapter 1

Introduction

This chapter provides a general overview of the project, the main goals to be achieved and the required specifications for the development and the implementation. It also includes a general work plan showing the project's organization.

1.1. General Overview

The combination of frequency-modulated continuous-wave (FMCW) technology and synthetic aperture radar (SAR) techniques leads to lightweight cost-effective imaging sensors of high resolution. FMCW SAR systems are playing an important role in airborne Earth observation fields, where frequent revisits at low cost are needed or where small size is a requirement. In fact, differently from pulse radars which require high peak of transmission power, FMCW systems operate with constant low transmission power, which means lower cost and smaller size[1]. On the other hand, the low transmitted power limits the maximum distance of interest to a few kilometres, which is, however, enough for several imaging applications.

Conventional SAR algorithms have been developed for pulse radars, therefore, when using FMCW sensors, proper algorithms have to be used to achieve the expected results with the maximum resolution. Under certain circumstances, in fact, the stop-and-go approximation used in conventional SAR algorithms is no longer valid.

The platforms UAV, like drones, is easy to understand that the flight path is not straight. This effect will introduce errors when the algorithm tries to reimage the scene that the UAV is covering. Also, a very important aspect is the Doppler effect. The radar sensor is onboard UAV, the motion will provide a Doppler that will introduce an error at the range determination that at the end will introduce a defocusing in the SAR image.

There are several algorithms to implement the SAR image formation:

- FFT Matched filter is one such method, which is used in majority of the spectral estimation algorithms, and there are many fast algorithms for computing the multidimensional discrete Fourier transform.[2]

- The APES (amplitude and phase estimation) method is also a matched-filter-bank method, which assumes that the phase history data is a sum of 2D sinusoids in noise.
- Backprojection Algorithm has two methods: Time-domain Backprojection and Frequency-domain Backprojection. The time-domain Backprojection has more advantages over frequency-domain and thus, is more preferred. The time-domain Backprojection forms images or spectrums by matching the data acquired from the radar and as per what it expects to receive. It can be considered as an ideal matched-filter for Synthetic Aperture Radar. [3]

The Backprojection is the algorithm that the project is going to study. The main advantage of Backprojection algorithm is the intrinsic precision since It matches the space/time filter. Using the information about the imaging geometry, a a pixel-by-pixel varying matched filter is obtained equalizing the changes suffered by the measured echoes back to each scattering point of the observed scene. On the other hand, the disadvantages are that it requires a higher computation effort compared to other approximate algorithms.

1.2. Project Goals

The goals of this projects are to implement a SAR algorithm based in the Backprojection algorithm. Also, before to compute the algorithm the project study the ways of generating the raw data that it is going to be processed. The study is composed by three steps:

- Generate raw data assuming the stop-and-go approximation and computing the Backprojection algorithm.
- Generate raw data without assuming the stop-and-go approximation and computing the Backprojection algorithm as the previous step.
- Finally generate raw data without assuming stop-and-go and applying the Backprojection algorithm assuming that the stop-and-go approximation is not applying in any case in this step.

Chapter 2

Frequency Modulated Continuous Wave Radar

In this chapter we will reproduce the main characteristics of the radars with FMCW technology, the data is extracted from the source [13].

2.1 Basic operating principles and theory

FMCW (Frequency Modulated Continuous Wave radar differs from pulsed radar in that an electromagnetic signal is continuously transmitted. The frequency of this signal changes over time, generally in a sweep across a set bandwidth. The difference in frequency between the transmitted and received (reflected) signal is determined by mixing the two signals, producing a new signal which can be measured to determine distance or velocity. A sawtooth function is the simplest, and most often used, change in frequency pattern for the emitted signal. FMCW radar differs from classical pulsed radar systems in that an RF signal is continuously output. Consequently, time of flight to a reflecting object cannot be measured directly. Instead, the FMCW radar emits an RF signal that is usually swept linearly in frequency. The received signal is then mixed with the emitted signal and due to the delay caused by the time of flight for the reflected signal, there will be a frequency difference that can be detected as a signal in the low frequency range.

Advantages

High resolution distance measurement

FMCW radars can have very high resolution for ranging, velocity and imaging application. Accuracy for non-moving targets is better than for moving targets and requires less processing power. Measurements of moving targets are of course possible but requires more powerful algorithms and hardware. Other technologies such as infrared or ultrasonics cannot detect range or only over very limited distances.

Performs well in many types of weather and atmospheric conditions

The short wave-length means that raindrops, water vapor or dust particles do not block wave propagation easily. Heavy rain is generally required before a reduction in range or resolution occurs. FMCW radars are also immune to effects from temperature differences, or high temperatures. systems will function identically during day or night. FMCW radars are also immune to effects from temperature differences, or high temperatures.

Good range compared to other non-radio technologies

Compared to systems operating in the visible or infrared light spectrum, or those using ultrasonic waves, FMCW radar sensors have excellent measurement range due to superior signal propagation.

Disadvantages

Reduced range compared to pulse radar

Due to the generally lower peak power output of FMCW radar systems, their long range performance can be lower than compared to pulsed systems. Since the transmitted signal is not as strong the received signal will be attenuated by atmospheric effects, interference, and distance. FMCW radars are however competitive to other competing technologies in range.

Susceptible to interference from other radio devices

Because they are continuously transmitting across a frequency band, FMCW systems may be more susceptible to interference from other electronic systems. This is due to the larger range of frequencies encountered and due to the lower “peak” power, resulting in the returned signal being overwhelmed by other emissions. Pulsed systems can generally overcome interference by increasing transmitted power or by switching frequencies. Distance measurement or detection systems using infrared, video, or lasers are generally immune to interference, given their operating principles.

Can require more computing power than pulse-Doppler systems

FMCW radar systems, given the need for high-quality fast Fourier transform processing to achieve accurate measurements, can require more advanced and powerful hardware. Given the continued decrease in computing cost, this is becoming less of an issue. However, the development and programming required can also be more complex, increasing costs.

2.2 Linear FM Signal

The signal model is defined as a linear frequency modulated signal, the schema below describes the signal processing and how the system generates the signal model. This model is going to use to generate the raw data.

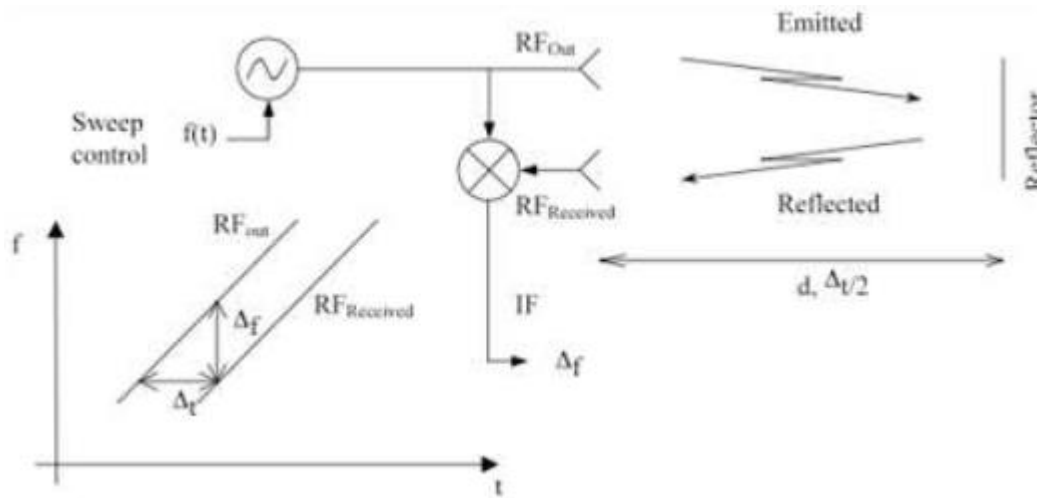


Figure 1. Schematic presentation showing how a low frequency signal is generated by mixing the received RF signal with the output RF signal. Due to the delay, Δt , caused by emitted signal traveling the distance to the reflector and back to the receiver, there will be a small difference in signal frequency between the two RF signals. This is output as an IF-signal with frequency Δf .

A simplified derivation of the intermediate frequency (IF) signal with the frequency Δf can be made in the following way: assume that the RF signal generator will output a frequency that is changing linearly over time as:

$$f_{RFout} = f_{RF0} + kf \cdot t, \quad 0 \leq t < T \quad (1)$$

Where f_{RF0} is the starting frequency, T is the frequency sweep time and kf is the slope of the frequency change, i.e. the sweep rate:

$$kf = \frac{BW}{T} \quad (2)$$

where BW is the frequency sweep bandwidth. The delay caused by the round-trip of the emitted signal to the reflector is calculated as:

$$\Delta t = 2 \frac{d}{c} \quad (3)$$

where d is the distance between the radar antenna and the reflector and c is the speed of light. Due to the delay, the frequency of the received signal compared with the emitted signal will be:

$$f_{RFrx} = f_{RF0} + kf \cdot (t - \Delta t), \quad \Delta t \leq t < T + \Delta t \quad (4)$$

The difference in frequency, Δf , between f_{RFrx} and f_{RF0} is thus:

$$\Delta f = kf \cdot (-\Delta t) \quad (5)$$

This is the signal that is output from the detector. The minus sign can be omitted since the real signal frequency output from the radar detector is wrapped to a positive frequency. Thus, the expression can be written as:

$$\Delta f = \frac{BW}{T} \cdot 2 \frac{d}{c} \quad (6)$$

2.3 Theoretical performance

The fundamental range measurement resolution of the system can be estimated as follows. The Fourier transform of a time limited signal can only detect an IF signal frequency with a resolution of $\frac{1}{T}$, keeping in mind that $\Delta t \ll \frac{1}{T}$; thus, the sampling time can be approximated by T . Using equation 6, this gives the minimum change in d , Δd , as:

$$\frac{1}{T} = \frac{BW}{T} \cdot 2 \frac{\Delta d}{c} \quad (7)$$

That it can be expressed as:

$$\Delta d = \frac{c}{2 \cdot BW} \quad (8)$$

The range measurement resolution is only limited by the sweep bandwidth. This is an important observation since it is saying that resolution is not dependent on the frequency of the RF signal itself, but rather only on the sweep bandwidth. There are methods of increasing the resolution of the measurements by a factor of 10 to 100 using fitting

algorithms. These find a peak in the IF signal spectrum which is not at an integer frequency point defined by the sampling rate and sweep bandwidth.

The range detection and FMCW radar principle may also be derived using a characterization of the IF signal phase rather than the frequency. This is recommended in order to understand the possibilities of a discrete system where the frequency sweep really is generated by a discrete set of frequencies. This derivation also lends itself more directly to high resolution range measurements.

2.4 FMCW radar principles using phase measurement, time discrete version

The RF signal will be radiated and reflected against a target. The echo is then received and compared (mixed) with the radiated RF signal. Had the system been measuring time-of-flight for a pulsed signal, the sensor output could be linear with distance. In an FMCW, however, the sensor output corresponds to the cosine of the phase difference between the echo signal and the radiated signal.

$$s = \cos(\theta) \tag{9}$$

Where s is the output signal from the sensor and θ denotes the phase difference between the echo RF signal and the radiated signal.

In other words, the measurement signal from the sensor will be a cosine signal indicating the round-trip electrical distance which the radiated signal has traveled.

$$s = \cos\left(2\pi \frac{2d}{\lambda}\right) \quad \text{where } \theta = \left(2\pi \frac{2d}{\lambda}\right) \tag{10} \tag{11}$$

Where d is the distance to the reflecting object and λ is the electrical wavelength of the RF signal. The multiplication by 2 accounts for the round-trip.

The expression for θ can also be written as:

$$\theta = \left(2\pi \frac{2d}{c} f_{RFout}\right) \tag{12}$$

The phase is developed:

$$\theta = \left(2\pi \frac{2d}{c}(fRF0 + kf \cdot t)\right) = \left(2\pi \frac{2d}{c}fRF0 + 2\pi \frac{2d}{c}kf \cdot t\right) \quad (13)$$

Once seen the development of the phase. The objective is to generate a beaten signal, that signal is generated following the following block diagram:

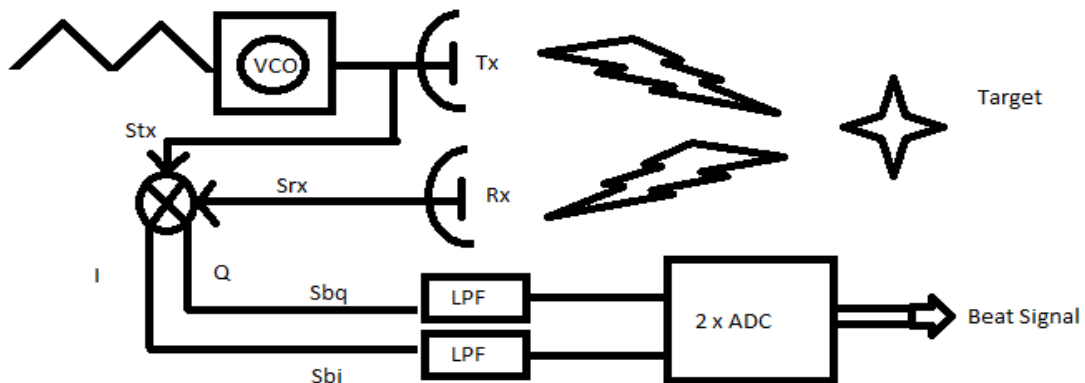


Figure 2 Bloc Diagram of quadrature demodulator. At the end of the chain the system is providing the beat signal.[4]

The system transmits an FM-Linear signal, that is, the incremental frequency while sweeping. The chirp signal is a good model to implement the system.

The development of the signal when it passes through the mixer and quadrature demodulator obtains a significant change in the phase. At the output of the ADC the beating signal is obtained, this signal is a tone at the frequency where the signal has bounced with the target. This frequency contains information about the distance between the radar and the target and the radial velocity of the target.

Mixer I/Q just analyzing the phase term.

$$Stx = \cos(\omega_0 \cdot t + \pi \cdot kf \cdot t^2) \quad (14)$$

$$Srx = \cos(\omega_0 \cdot (t - \Delta t) + \pi \cdot kf \cdot (t - \Delta t)^2) \quad (15)$$

- I Branch

$$\begin{aligned} S_{bi} &= \cos(\omega_0 \cdot t + \pi \cdot kf \cdot t^2) \cos(\omega_0(t - \Delta t) + \pi \cdot kf \cdot (t - \Delta t)^2) = \\ &= \cos(-\omega_0 \cdot \Delta t - 2\pi \cdot kf \cdot \Delta t \cdot t + \pi \cdot kf \cdot \Delta t^2) \end{aligned} \quad (16)$$

- Q Branch

$$\begin{aligned} S_{bq} &= \cos(\omega_0(t - \Delta t) + \pi \cdot kf \cdot (t - \Delta t)^2) \sin(\omega_0 \cdot t + \pi \cdot kf \cdot t^2) = \\ &= \sin(-\omega_0 \cdot \Delta t - 2\pi \cdot kf \cdot \Delta t \cdot t + \pi \cdot kf \cdot \Delta t^2) \end{aligned} \quad (17)$$

- DEM I/Q Output

$$S_b = e^{-j(-\omega_0 \cdot \Delta t - 2\pi \cdot kf \cdot \Delta t \cdot t + \pi \cdot kf \cdot \Delta t^2)} \quad (18)$$

Phase terms:

- $\omega_0 \cdot \Delta t$: Phase is changing due to the range between radar and target.
- $2\pi \cdot kf \cdot \Delta t \cdot t$: Beating tone, the tone frequency that the receiver read.
- $\pi \cdot kf \cdot \Delta t^2$: Residual video phase (RVP)

It can be rejected if $\omega_0 \cdot \Delta t \gg \pi \cdot kf \cdot \Delta t^2$

Finally, the signal model is (18)

$$S_b = e^{-j(-\omega_0 \cdot \Delta t - 2\pi \cdot kf \cdot \Delta t \cdot t + \pi \cdot kf \cdot \Delta t^2)}$$

This model is going to use to generate the raw data. The phase is going to be the most important term. This kind of signal, linear FM, can be represented frequency vs time domain. This representation allows us to understand how the signal is changing due to the scene that the transmitter is transmitting signal.

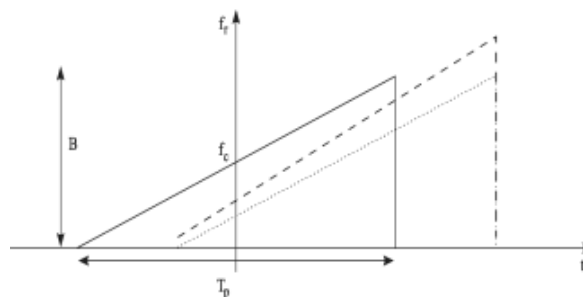


Figure 3 This is the beat signal, T_p is the time duration of each frequency pulse. The reference is the ramp with continuous line and the Doppler effect is observed in the dashed line, that the frequency is changing.

2.5 Pulse Compression FMCW

The general concept of pulse compression is to generate a signal with energy content of long-duration, low-power pulse will be comparable to that of the short-duration, high-power pulse.

To determine a range the compression is critical to determine the range resolution because it will be defined by the resolution of the compressed pulse. The pulse compression, also called range compression when it is talking in SAR algorithms, can be computed by fast Fourier transform. The FFT can be understand as a matched filter, that will provide the compression in frequency domain. The resolution will depend on the number of samples of FFT.

Chapter 3

Synthetic Aperture Radar Concepts

The principle of SAR is based on the phase history of the echoes that the radar is collecting while it is pointing to a scene. The phase history is processed to reimage the scene that the radar was pointing. The SAR is defined by specific geometry. The geometry has two important faces, Range and Azimuth they correspond to the 2D-image that SAR algorithm form.

3.1 SAR Geometry

The general geometric model is described in the figure below. The sensor is placed at the UAV and is moving following the flightpath.

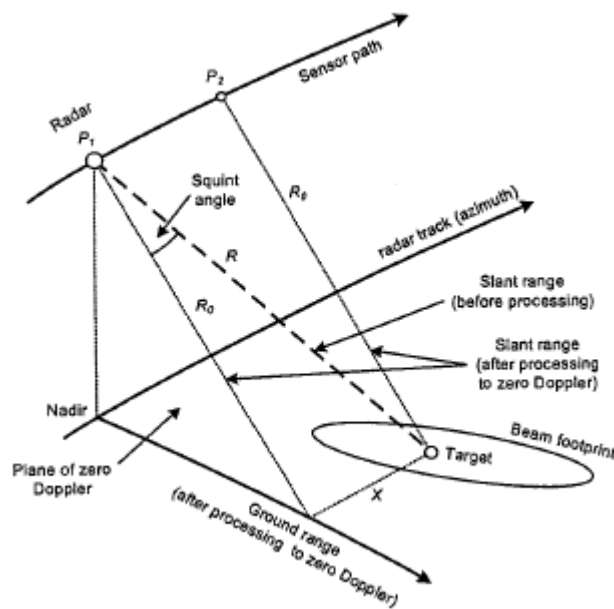


Figure 4 SAR geometric model

Radars system can be monostatic, bistatic or multistatic, depending upon the location of the receiver in relation to the transmitter. A monostatic radar, in which the same radar antenna is used for transmission and reception is assumed to define the terms to describe de SAR geometric model.

- The target is a point placed ant the Earth's surface that the SAR system is imaging. This point is called also *point scatterer*.
- The beam footprint is the illumination of the antenna radar, while the UAV is moving around the sensor path de beam footprint is changing at the same time.
- In SAR context, this a direction aligned with the relative platform velocity vector. It can be considered as vector parallel to the sensor motion.
- The platform velocity, the UAV speed relative to the Earth.
- Zero Doppler plane, is the plane containing the sensor that is perpendicular to the platform velocity vector. The intersection of this plane with the ground is called the zero Doppler line. When this line crosses the target, the relative radial velocity of the sensor, with respect to the target, is zero.
- The distance from the radar to the target varies with time as the UAV moves. When the range is minimum, when de zero Doppler line crosses the target, it is called the range of closest approach.

There are two dimensional spaces used for the SAR data in the signal processor. The signal space contains the received SAR data, and the image space contains the processed data. If the data in the signal are displayed, features imaged by the radar are not recognizable. The features will emerge only after extensive processing is preforming on the input data.

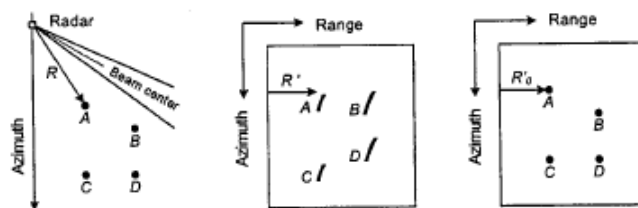


Figure 5 SAR processing: raw data, range compression and azimuth compression

3.2 SAR Range equation

The single most important parameter in SAR processing is the range between radar to target. As the sensor approaches the target through the motion of the radar platform, the range decreases with every pulse. After sensor passes the target, the range increases with every pulse. This change in range has important implications. It causes phase modulation from pulse to pulse, which is necessary to obtain fine azimuth resolution in the SAR processor. This results in a hyperbolic form of range equation.

Chapter 4

Development: SAR Backprojection Algorithm

In this chapter we explain the different developments of algorithms, based on the image reconstruction algorithm Backprojection. These algorithms have been developed in the Matlab environment.

The geometry of the study is designed as follows:

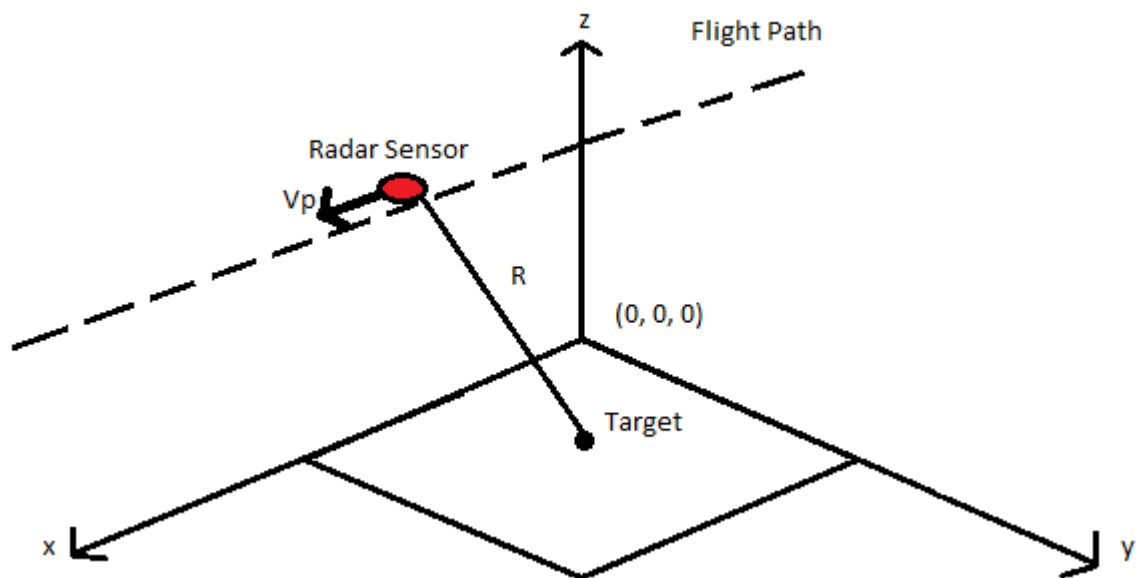


Figure 6 SAR geometric model Case 1,2,3

The platform where the radar is located, moves on the axis x , in the azimuthal direction. The axis that follows the direction y , is the range axis. The square is the scene that the radar will capture the echoes from it. Finally, the point located in the centre of the scene is the target.

All the cases of studies are structured in the same way. First, the system parameters are defined. Next, the simulation of the scene is carried out, that is, the acquisition of data according to the case study being carried out. At this point, the signal model to be processed is defined. Once the data has been obtained, it will be processed to compress it in the range direction. Next, the compressed data is treated by the Backprojection algorithm, applying the reconstruction according to the case study.

The input parameters of the system are the following:

c	Speed of Light
f0	Carrier Frecuency
Vp_max	Max Platform's speed
Rmax	Maximum Range
dR	Range resollution
L	Length Synthetic Aperture

Table 1 System Inputs

The parameters of [T1] derive the calculation of other parameters that condition the case study.

$$\lambda = \frac{c}{f_0}, [\text{m}] \quad (19)$$

$$fDopp_max = \frac{2}{\lambda} Vp_max, [\text{Hz}] \quad (20)$$

$$BDopp = 2 \cdot fDopp_max, [\text{Hz}] \quad (21)$$

$$SRF = 2 \cdot Bdopp, [\text{Hz}] \quad (22)$$

$$Tm = \frac{1}{SRF}, [\text{s}] \quad (23)$$

$$df = \frac{c}{2dR}, [\text{Hz}] \quad (24)$$

$$\alpha = \frac{df}{Tm}, [\text{Hz/s}] \quad (25)$$

$$fr_max = \frac{2 \cdot Rmax \cdot df}{Tm \cdot c}, [\text{Hz}] \quad (26)$$

$$fb_max = fr_max + fDopp, [\text{Hz}] \quad (27)$$

$$fS_{Ny} = 2 \cdot fb_max, [\text{Hz}] \quad (28)$$

$$fs = 4 \cdot fS_{Ny}, [\text{Hz}] \quad (29)$$

The Doppler bandwidth is defined as twice the maximum Doppler frequency. This maximum Doppler frequency is conditioned by the maximum speed of the Platform. Observing the definitions of the Doppler bandwidth it is concluded that the maximum speed of the platform conditions the SRF, the parameter that describes the repetition of ramps radiated by the radar. Define [25] as sweep frequency. Equation [26] describes the

maximum beat frequency due to the distance to the object located in the scene. Finally, the sampling frequency is defined [29]. The sampling frequency is defined by going over the Nyquist limit so as not to introduce aliasing problems.

The vector t is defined so that the duration, T_m , of the frequency ramps can be sampled at the sampling frequency of the system.

In all the cases of studies a reconstruction of an image will be carried out where its dimensions will be 100 meters in range and 100 meters in azimuth. The case studies are going to be done with a target located in the center of the scene.

4.1 Case 1: Stop-and-Go

The first case study is based on creating an algorithm, where the data is generated using the stop-and-go approach. Afterwards the data is processed by applying the frequency compression to finally apply the Backprojection algorithm with the correction of the phase taken into account that the data has been generated with the approach of stop-and-go.

The radar will fly over the scene following the flight path, while it will capture the RF signals that reflect on the scene. In order to model this situation, the stop-and-go approach is introduced. The model is based on jumping the radar, that is, the axis is sampled, where the platform moves, by observations. Samples of the echos of the scene are collected for the position of each observation, until completing the course of the platform. In this way we do not take into account the motion that the platform performs between observation and observation. This allows to simplify the algorithm, but it conditions the parameters in which the radar must act to advise to focus accurately on the image that will be generated, when processing the data captured by the radar.

The input parameters that have been used for this first case study are the following:

c	Speed of light	3e10 [m/s]
f0	Carrier Frequency	10e9 [Hz]
Vp_max	Max Platform's speed	80 [km/h]
Rmax	Maximum range	150 [m]
dR	Range Resolution	1 [m]
L	Length of synthetic Aperture	4 [m]

Table 2 Input parameters Case 1

The target is placed in the position (50; 50; 0), meters. The parameter L, of the table [T2], defines the length of the synthetic aperture. This means that it defines the initial position of the radar. The radar performs a symmetrical azimuth sweep. This means that with the position of the target and the parameter L [T2], the initial position of the radar (48; 0; 0), meters, is defined. The synthetic aperture is defined as 4 meters; therefore, the radar will perform a sweep on the azimuth axis from (48; 0; 0) to (52; 0; 0).

This sweep must be discretized in observations, that is, to model it we must divide these 4 meters of radar flight. The division is made in such a way that for each observation the radar radiates a frequency ramp. This means that, depending on the speed of the platform and the duration of each ramp, the number of observations is defined, *Nobs*.

Once you have defined the number of observations, define the matrix where the data is stored. The matrix is defined with dimensions (*Nobs* X length (t)). The simulation of raw data is done through iterations, where each iteration corresponds to an observation. The loop is based on, performs an update of the radar position. Next, the time it takes for the radiated wave to reflect on the target and return to the radar is calculated. The calculation of the delay time is an essential parameter to perform detections on the range of axes.

$$\tau = \frac{2 \cdot \text{distance}}{c}, [\text{s}] \quad (30)$$

Where, $\text{distance} = \sqrt{(\text{radar}_{\text{posx}} - \text{target}_{\text{posx}})^2 + (\text{radar}_{\text{posy}} - \text{target}_{\text{posy}})^2 + (\text{radar}_{\text{posz}} - \text{target}_{\text{posz}})^2}, [\text{m}]$ (31)

Then the beating signal is generated, this signal models the signal at the output of the mixer:

$$s = e^{-j(-\omega_0 \cdot \tau - 2\pi \cdot \alpha \cdot \tau \cdot t + \pi \cdot \alpha \cdot \tau^2)} \quad (32)$$

The signal is saved in the position of the corresponding observation.

After generating raw data, the matrix where those data are stored is composed of tones, one in each row. These are tones at the beat frequency, which correspond to the distance at which the target is located. As for the phase, it is a linear phase that oscillates between π and $-\pi$.

In the following figure [F6] the tone that has been generated at the output of the radar mixer is observed. On the other hand, in [F7] the phase is observed in the same observation (PCA). The result shows the oscillation between π and $-\pi$ and its linear behavior.

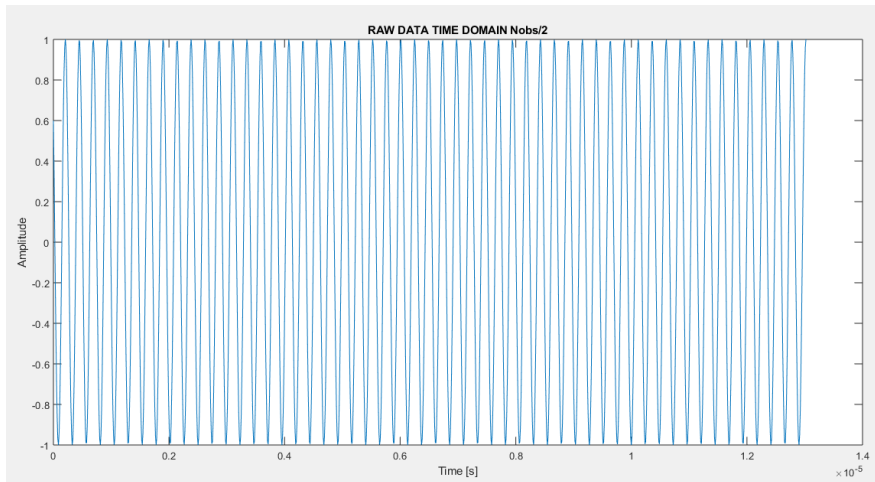


Figure 7 Time domain, Raw data at the point of closest approach (PCA)

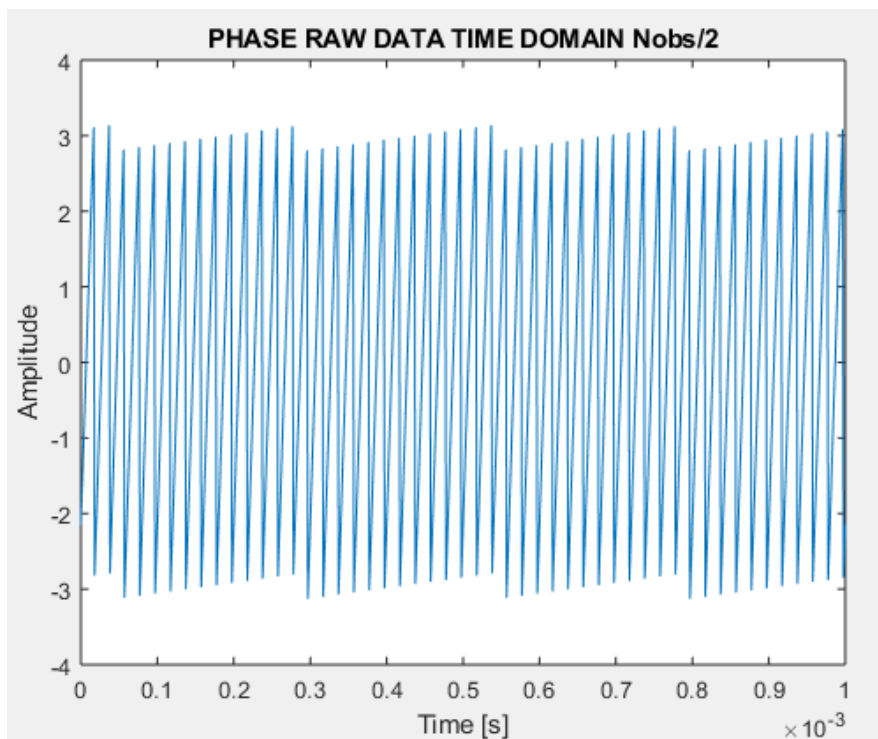


Figure 8 Time domain, Raw data phase the point of closest approach (PCA)

The next step is the compression of the tones in the frequency domain. To carry out this process, a Fast Fourier Transform is applied to each of the rows of the raw data matrix. To

perform the FFT, the number of samples large enough to obtain a well-defined sync function is defeated.

The image of the matrix of the compressed data is shown in the following figures. It is observed how a sync function is formed that forms an arc shape that belongs to when the platform approaches the target and then turns away. The phase of the signal is parabolic.

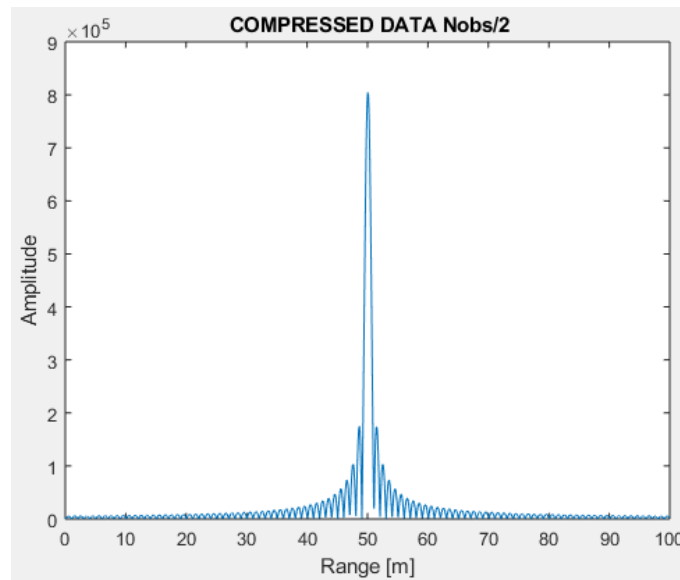


Figure 9 Frequency domain, compressed data at the point of closest approach (PCA)

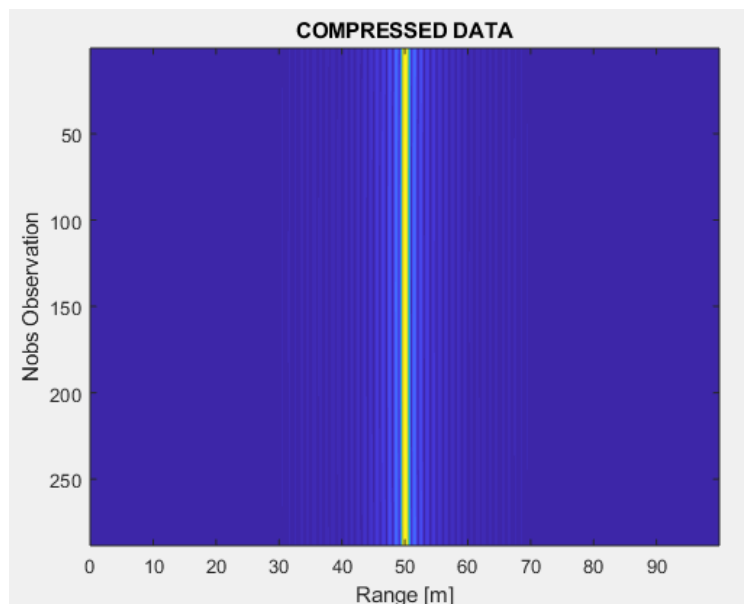


Figure 10 Frequency domain, compressed data image of all observations

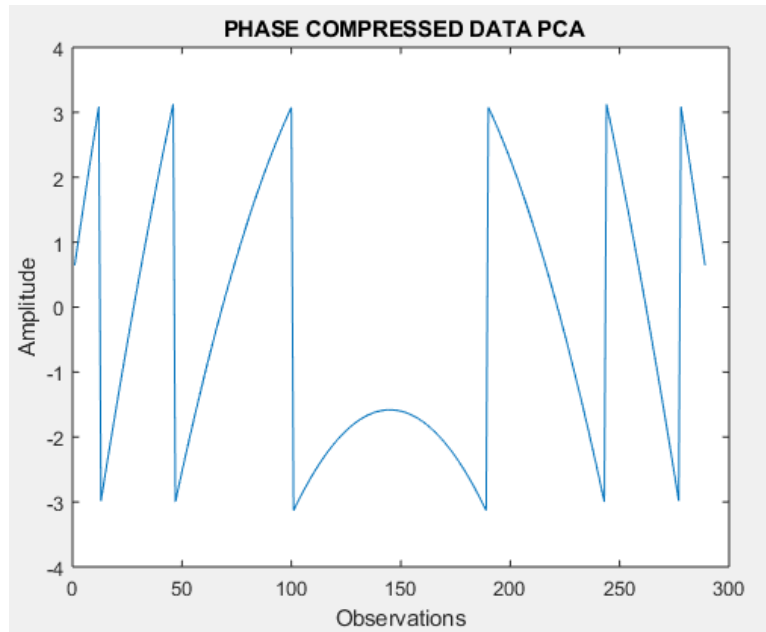


Figure 11 Frequency domain, phase compressed data at PCA

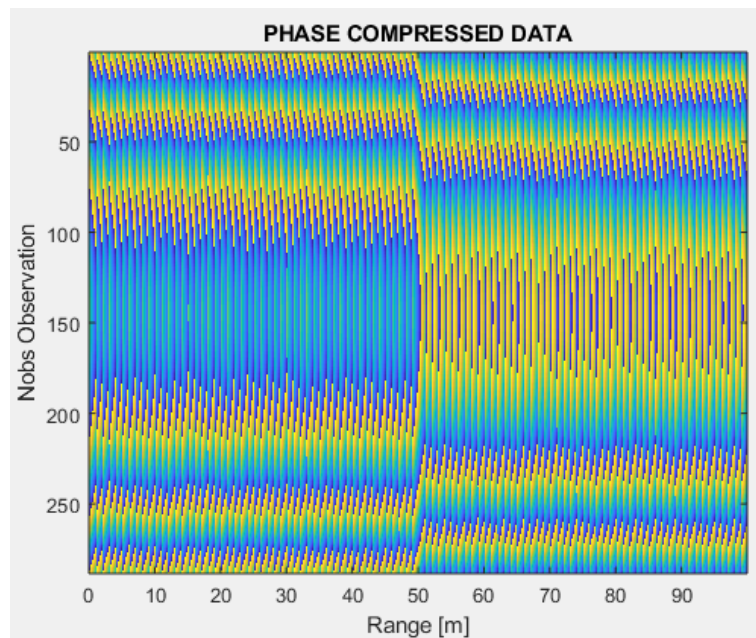


Figure 12 Frequency domain, phase compressed data image of all observations

With the compressed data stored in the data matrix. The next step is to apply Backprojection. First an empty matrix is created, where the data processed by the Backprojection will go, that is, the final image. This matrix of dimensions $(100 \times 100 \cdot ntf)$.

In the range axis, the frequency step must be taken into account. To be able to calculate distances in the correct units. The variable ntf corresponds to:

$$ntf = \frac{nfft}{length(t)} \quad (33)$$

The algorithm to reconstruct the image is based on traversing the empty matrix pixel by pixel. Within each pixel, the distance between the pixel and the radar is calculated for each observation.

This distance between the pixel and the radar is an important parameter and careful to calculate the distances in the correct units. Next, the distance between the pixel and the radar in the compressed data matrix is calculated. Most of the cases will not be a sample that exists and should be interpolated. A linear interpolation is made to decide which sample of the compressed data matrix fits the distance, between pixel and radar, in meters. The value of that sample obtained in the interpolation is applied a phase correction. That phase is equivalent to:

$$e^{j2KR}, \text{ where } R \text{ belongs to the distance between pixel and radar} \quad (34)$$

The result of the correction is stored in a variable in which a cumulative sum of the process is made for each observation. Once it has been made for all observations, the result of that cumulative sum of phase corrections is the final value for that pixel.

In the following image shows the reconstruction of the scene. The target located in the center of it is observed.

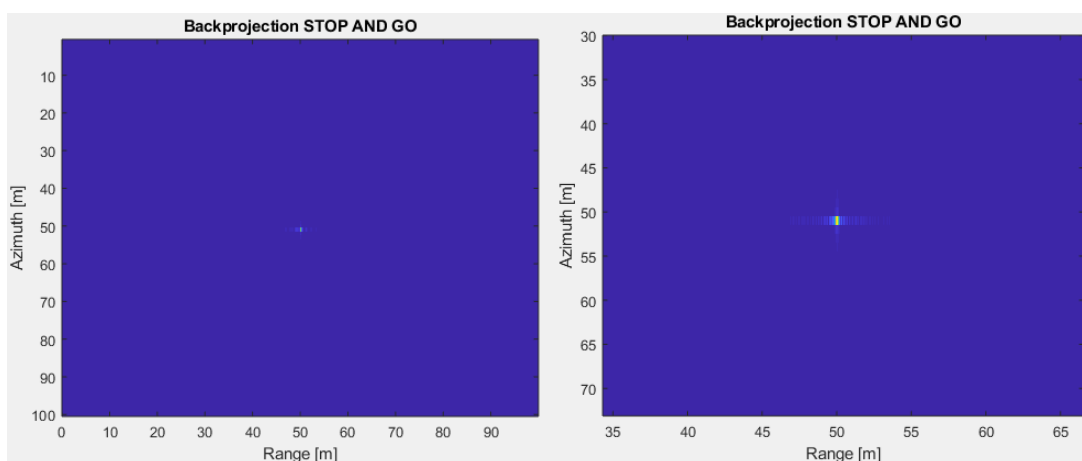


Figure 13 Backprojection algorithm. It is the same case but right side with zoom.

Cutting on both axes :

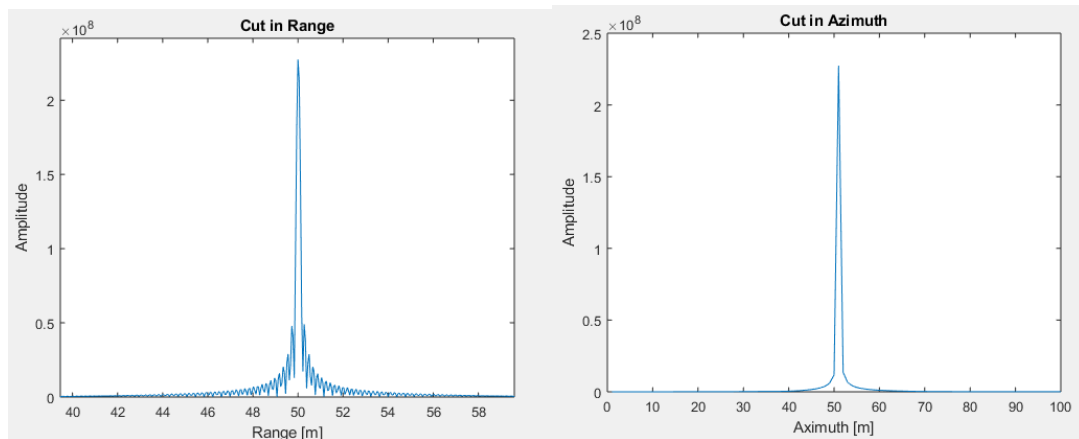


Figure 14 The cuts on Range and Azimuth axis.

4.2 Case 2: Non-Stop-and-Go

In the second case study, the generation of raw data will be treated without assuming the stop-and-go approach. The idea is based on taking into account the motion of the platform between observations. From the point of view of the radar it can be interpreted that the target is the one that is in motion while the radar remains still. With this interpretation, the radial velocity observed by the radar coming from the target causes disturbances in the calculation of the time it takes for the signal to return to the radar.

The main idea of this case study is to observe the blurring that occurs when not applying the stop-and-go assumption. That is why comparisons are going to be made between the first and the second case. The final result of this study is observed when the Backprojection algorithm is applied without taking into account that the data has not been generated assuming stop-and-go. The final SAR image that is generated is out of focus.

The parameters used for this case are the same as in the previous case, [T2]. The geometry is maintained with respect to the previous case, the radar continues to jump along the x axis, but this time when the time it takes for the signal to reflect and return to the radar is calculated, the radial speed observed by the radar is taken into account about the target.

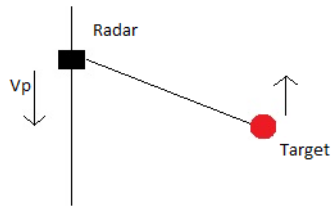


Figure 15 Interpretation where the radar is the object that is still and the target that is moving.

To calculate the time it takes the signal is modeled taking into account that when the radar passes just ahead of the target (PCA), the radial speed is 0, therefore, the result of that observation with respect to the previous case is the same. The defocus is introduced by the rest of the observations since the radial velocity introduces a displacement effect in frequency. To generate raw data the same algorithm is used as in the previous case except the calculation of the time taken by the signal. This time delay is calculated as follows:

$$\tau = \frac{2}{c} \left(radar2target + \left(vp \left(1 - \frac{radar_posx}{radar2target} \right) \right) \right), [s] \quad (35)$$

The signal model is exactly the same as in the first case. That is, a tone at a certain frequency, according to the observation. All the tones received by the radar are stored in a raw data matrix.

The next step is to compress the generated data. The processing is through a Fast Fourier transform. The compressed data is stored in a matrix. Where each row corresponds to the compressed tone in the form of sync. In this, a comparison is made to observe the behavior of generating the data without applying the stop-and-go approach.

The following figure shows a data matrix where the data generated in the first case and the data generated in this second case are merged. It is observed that at the point where the radar is in the position closest to the target the result is the same. On the other hand, the radar moves away from that position and an error is introduced in the compression range.

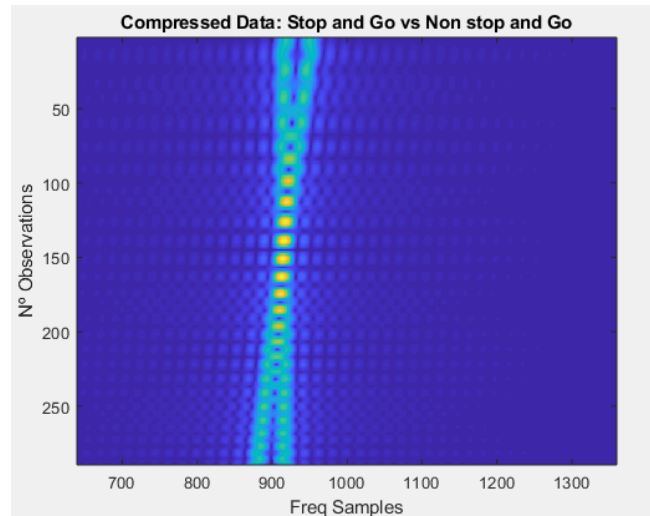


Figure 16 Compressed data stop-and-go vs nonstop-and-go. It can be observed that in the central point of the synthetic transport the result is the same in the two cases because the radial velocity is 0.

The last step is the reconstruction of the scene. To carry out this last step, the Backprojection algorithm is applied in the same way as in the first case. The phase correction will not consider that the stop-and-go approach is not applied, therefore a defocus is introduced.

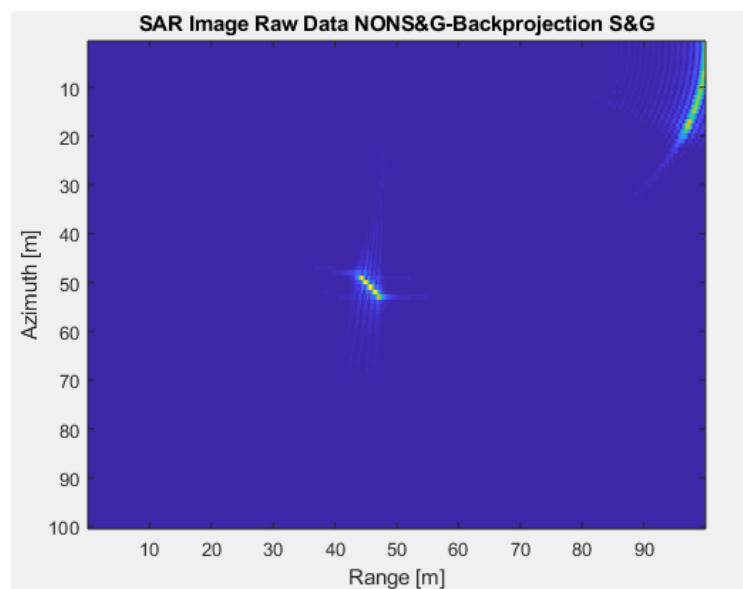


Figure 17 In the execution of the Backprojection, the non-application of the stop-and-go approach is not taken into account and a blur is introduced in the image.

4.3 Case 3: Backprojection correction for non stop-and-go

The last case study aims to correct this blurring that occurs when applying the Backprojection algorithm in the previous case. The blurring is produced in the correction of the phase that the Backprojection applies. In the phase correction, it must be taken into account in which way the data has been generated. Therefore, the phase change introduced when generating raw data without assuming stop-and-go must be accounted. The correction of the phase applied in the first and second cases follows the formula (34). To focus the image in this case we introduce the term that corresponds to the radial velocity observed by the radar on the object.

$$e^{j2KR + \left(vp \left(1 - \frac{\text{radar_posx}}{\text{radar2target}} \right) \right)}, \text{ where R belongs radar to pixel distance} \quad (36)$$

In this way the result of the SAR image is as follows:

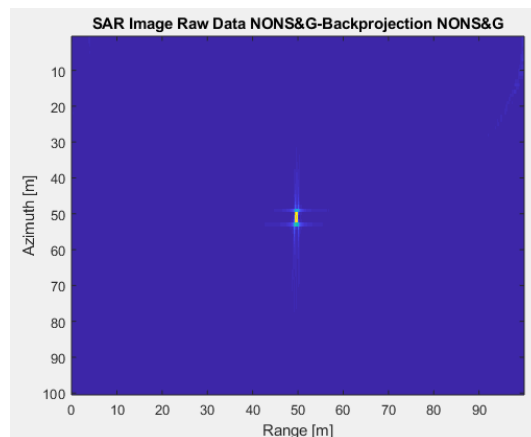


Figure 18 Backprojection algorithm without stop-and-go approximation.

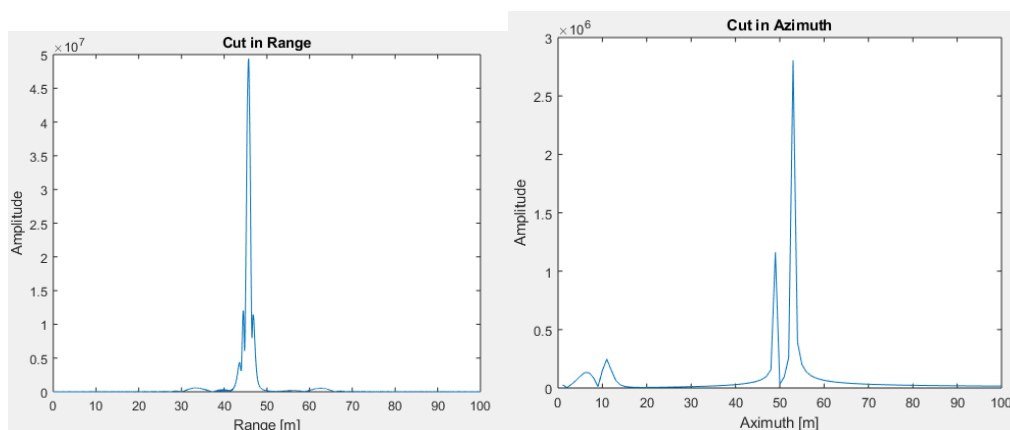


Figure 19 Backprojection algorithm without stop-and-go approximation. Cuts in Range and Azimuth.

Chapter 5

Conclusions and future work

In this thesis, we wanted to carry out a study on the capabilities of generating images through radar technology, more precisely, the FMCW technology. An algorithm design has been proposed to form synthetic radar apertures assuming the stop-and-go approach. For this, a data model and a series of parameters that model the scenario have been presented. With this case resolved, an attempt has been made to combat the problem without using the stop-and-go approach. The results obtained are not optimal, but the perturbation introduced by not using the stop-and-go approach has been reversed.

During the whole process of the project, many obstacles have appeared, the learning curve has been slow, but ascending. All the documentation and theory about synthetic openings and FMCW technology has been complicated to transfer it to a Matlab code.

As work for the future, it would be convenient to try to adjust the resolution of the approaches of the algorithms. A future improvement would be to model the code so that you do not have to use loops to perform the calculations.

Bibliography:

- [1] Liu, Y & Deng, Yun-Kai & Wang, Robert & Yan, Hongsong & Chen, J. (2012). Efficient and precise frequency-modulated continuous wave synthetic aperture radar raw signal simulation approach for extended scenes. *Radar, Sonar & Navigation, IET*. 6. 858-866. 10.1049/iet-rsn.2011.0288.
- [2] Y. C. Lee, V. C. Koo and Y. K. Chan, "Design and development of FPGA-based FFT Co-processor for Synthetic Aperture Radar (SAR)," 2017 Progress in Electromagnetics Research Symposium - Fall (PIERS - FALL), Singapore, 2017, pp. 1760-1766.
- [3] J. Moll and V. Krozer, "Time-varying inverse filtering of range-compressed radar signals," 2012 The 7th German Microwave Conference, Ilmenau, 2012, pp. 1-4.
- [4] A. Meta, P. Hoogeboom and L. P. Ligthart, "Non-linear Frequency Scaling Algorithm for FMCW SAR Data," 2006 European Radar Conference, Manchester, 2006, pp. 9-12.
- [5] A. Meta, P. Hoogeboom and L. Ligthart, "Range Non-linearities Correction in FMCW SAR," 2006 IEEE International Symposium on Geoscience and Remote Sensing, Denver, CO, 2006, pp. 403-406.
- [6] W. G. Carrara, R. S. Goodman, and R. M. Majewski, *Spotlight Synthetic Aperture Radar*. Boston, MA: Artech House, 1995.
- [7] Z. Zhu, W. Yu, X. Zhang, and X. Qiu, "A correction method to distortion in FMCW imaging system," in *Proc. IEEE NEACON*, Dayton, OH, May 1996, pp. 323-326.
- [8] V. T. Vu, M. I. Pettersson and S. Björklund, "A method to implement SAR slow-time step in beamforming stage of fast backprojection algorithm," 2014 IEEE Geoscience and Remote Sensing Symposium, Quebec City, QC, 2014, pp. 3686-3689.
- [9] C. Trampuz, A. Meta, A. Coccia and E. Imbombo, "MetaSensing - the advanced solution for commercial and scientific SAR imaging," 2012 Tyrrhenian Workshop on Advances in Radar and Remote Sensing (TyWRRS), Naples, 2012, pp. 326-329.
- [10] L. Chun-Yang and J. Yong-Chang, "SAR echo-wave signal simulation system based on MATLAB," 2012 International Conference on Microwave and Millimeter Wave Technology (ICMMT), Shenzhen, 2012, pp. 1-4.
- [11] A. Broquetas, "GEOSAR Backprojection", personal papers.
- [12] Ian Cumming and Frank Wong (2005) *Digital Processing of SAR Data*. Artech House, Norwood, MA
- [13] Sivers IMA AB, "FMCW Radar Sensor Application Notes" 2011 SE-164 29 Kista, Sweden

Glossary

- **SAR** Synthetic Aperture Radar
- **FMCW** Frequency modulated continuous wave
- **UAV** Unmanned aerial vehicle
- **FM** Frequency modulated
- **APES** Amplitude and Phase estimation
- **RF** Radiofrequency
- **BP** Backprojection
- **S&G** Stop and Go
- **DEM** Demodulator
- **SRF** Sweep repetition frequency